

Investigation on Delamination Damage of a Composite Cross-Joint

Tienan Cao*, Jixing Yang, Fusen Ji

AECC Shenyang Engine Research Institute, Shengyang 110015, China

Abstract: The reliability of the joint structure greatly restricts the application of composite materials in aeroengines. And the delamination damage is the main factor restricting the reliability of the joint structure. In this paper, in view of the joint structure characteristics of engine fan/ compressor blade, adjustable blade and other components, a kind of composite cross-joint structure is proposed, and the 9 layer schemes under symmetrical and asymmetric two designs is given. Through the establishment of a detailed finite element analysis model, the delamination damage and influence of delamination damage on the bending stiffness of cross-joint under the equivalent aerodynamic load are analyzed. Finally, the delamination damage and changing of cross-joint blending stiffness in the 9 design schemes are compared and analyzed.

Keywords: resin matrix composites joint; delamination damage; structure stiffness; Fans/compressor blade; adjustable vane.

1 Introduction

With the growing maturity of composite manufacturing technology, the application of composite materials on aero-engine components has a great tendency to replace metal materials. At present, the resin matrix composites have been widely used in aero-engine fans, casing and other structures. With the progress of the technology of high temperature resistant resin matrix composites, the composite structure is widely applied in fan booster stage and compressor. The structures of aero-engine fan booster stage and compressor have complex structure and complicated load conditions. While, how to solve the connection of different components and the reliability of connection structure are always difficult to solve. The usual mechanical connection will lead to the cutting off of the composite fiber and greatly reduce the bearing capacity of the composite material.

The integrated composite structure can not only reduce the number of parts, reduce the additional mass of joints and transition zone ^[1], but also reduce the damage caused by mechanical joints. The keys of integrated composite structure design are how to realize the connection of multiple structural units, under the joint have the sufficient bearing capacity, the continuity of the transmission path ^[2].

*Corresponding author: (jasoncao1987@126.com)

According to the different form of connected structures, the composite joints can be divided into two kinds, including planar joints and non-planar joints^[3]. Due to the complexity of the damage form, the studies of non-planar composite joints are performed under single load, such as tensile, bending and shear. The T-shaped, L-shaped and π -shaped composite joints are focused on^[4]. On the aero-engine, the non-planar composite joints are usually used on the composite fan blades without platforms, and are adopted as the connecting structure of blades and tenons. However, the fan blades under the working conditions are usually subjected to various loads such as centrifugal force and aerodynamic force, which may make the loads of the composite joints complicated.

Delamination damage is a typical failure mode of the composite non-planar joints, which often occurs before the failure of fiber fracture, matrix cracking, fiber pull out and so on. So delamination damage of composite joints is the important factor, which limits the bearing capacity of composite structure. Numerous of investigations into the structural properties of composite T-joints have shown that the weakest location is the resin fillet and radius bend region^[5-20]. The finite element and experimental studies of the T-joint on the mechanical properties under tensile load have shown the T-joint structure failure process. At the initial stage of structural failure, the cracking firstly appears in the resin fillet. As the increasing of the load, the cracking spreads into the surrounding plies and causes delamination. Delamination cracking between the plies and resin fillet usually cause significant loss of bearing capacity, and often defines the maximum operating load and strain limit to T-joints. Finally, fiber and matrix damage gradually occurred in the laminate^[19]. The damage process of π -joint and L-joint structures are similar to the T-joint structure, and the delamination directly affects the structural bearing capacity. Therefore, the study of delamination is very important for the joint structure design of non-planar composite materials.

Some composite aero-engine parts are complicated in structure and usually acted by aerodynamic loads and mechanical loads, such as fans/compressor blade with tenons, adjustable vane, and casing with reinforcement rib. The force forms are complex, so the conventional T-joint, π -joint and other connecting structures are unable to realize the geometric structure, strength and stiffness requirements. In view of the above requirements, a kind of cross shape composite connection structure is proposed in this paper, which can be used to connect four composite components at the same time, and satisfy the structural form of the fans/compressor blade with tenons, adjustable vane and so on. On this basis, the influence of the different lay-up on the laminates and different laminate orientations in four sub-parts on the cross-joint is investigated, under the effect of the equivalent aerodynamic bending moment.

2 Cross-joint model

The composite cross-joint structure is divided into laminate areas and filling area (as shown in Fig.1). The laminate areas include the left upper area (UL area), the left

lower area (DL area), the right upper area (UR area), the lower right area (DR area), and the middle area (M area), all made of T700/TDE-85 composite unidirectional prepare. The M area is used to increase the twist strength of the connection structure when the connected component is subjected to aerodynamic loads, so as to prevent the delamination. The mechanical properties of unidirectional T700/TDE-85 laminate are shown in Table 1 and table 2. The filling areas include the left filling area (FL area) and right filling area (FR area), all made of resin. The elastic modulus of Cured resin is $E=50GPa$ and Poisson's ratio is $\gamma =0.3$. The area ensures the geometry of the cross-joint structure and prevents fiber breakage.

Table 1. The elastic modulus of the unidirectional T700/TDE-85 laminate^[5]

E_1	E_2, E_3	r_{12}, r_{13}	r_{23}	G_{12}, G_{13}
134 GPa	9.6 GPa	0.29	0.3	4.8 GPa

Table 2. The Strength of the unidirectional T700/TDE-85 laminate^[5]

X_t	X_c	Y_t	S_{12}, S_{13}	S_{23}
2097 MPa	1258 MPa	42 MPa	119 MPa	83.7 MPa

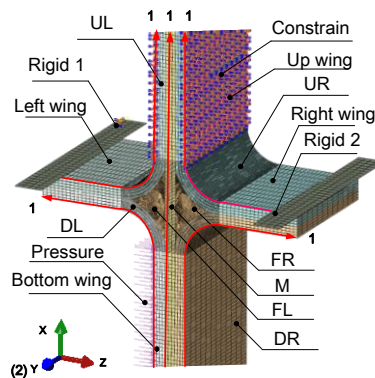


Fig.1. The composite cross-joint structure

According to the actual working conditions of the cross-joint structure in the aero-engine, the boundary conditions and loads are simplified, see Fig1. The boundary conditions applied to the FE model of the cross-joint involved clamping the skin on up wing, the clamped rigid 1 and rigid 2 are used to constrain the x direction displacement of the left wing and right wing, by applying contact interaction. The equivalent aerodynamic load of 1MPa is applied to the skin of the bottom wing. The laminate area (UL area, UR area, DL area, DR area and M area) and filling area of the cross-joints are constructed as a 3D model using C3D8I solid elements. Quadratic stress criterion is used as the initial damage model of cohesive mode, and Benzeggagh-Kenane fracture criterion is used as damage evolution model^[4], the parameters of the cohesive model are shown in **Table 3**.

Table 3. Parameter of cohesive model

Parameter	E_{33}/Mpa	G_{13}/Mpa	G_{23}/Mpa	G_{1c}/J	G_{IIc}/J
Value	10000	10000	10000	0.105	3
Parameter	G_{IIIc}/J	t_n^0/MPa	t_s/MPa	t_r/MPa	η/I
Value	3	10	15	15	1.75

3 The designs and analysis of T-joints

3.1 Laminates designs of designing laminates

In order to investigate the influence of composite laying method on the cross-joint, this paper gives nine series designs of composite cross-joint (as shown in Table 4). The coordinate system of each laminate is discrete coordinate system, and its main direction (axis 1) is along the long side of each laminate, shown in Figure 1. The axis 2 is the Y axis of the global coordinate system, and the axis 3 is the lay-up direction. According to the layer direction of the left area (UL area and DL area) and the direction of the right area (UR area and DR area), the nine series designs are divided into two types: symmetrical laying (case I) and asymmetric design (case II), taking the laminate of M area as the symmetric surface. All the laminates in the M area are designed to be 0° , in order to ensure the connection strength between up wing and bottom wing of the cross-joint, eliminate the coupling stiffness of the symmetric surface (M area), simplify the designs of laminates in other areas.

Table 4. Layer scheme of composite cross-joint

		UL area	DL area	M area	UR area	DR area
Case I	1	$(0^\circ)_4$	$(0^\circ)_4$	$(0^\circ)_3$	$(0^\circ)_4$	$(0^\circ)_4$
	2	$(15^\circ)_4$	$(15^\circ)_4$	$(0^\circ)_3$	$(15^\circ)_4$	$(15^\circ)_4$
	3	$(30^\circ)_4$	$(30^\circ)_4$	$(0^\circ)_3$	$(30^\circ)_4$	$(30^\circ)_4$
	4	$(45^\circ)_4$	$(45^\circ)_4$	$(0^\circ)_3$	$(45^\circ)_4$	$(45^\circ)_4$
	5	$(60^\circ)_4$	$(60^\circ)_4$	$(0^\circ)_3$	$(60^\circ)_4$	$(60^\circ)_4$
	6	$(75^\circ)_4$	$(75^\circ)_4$	$(0^\circ)_3$	$(75^\circ)_4$	$(75^\circ)_4$
	7	$(90^\circ)_4$	$(90^\circ)_4$	$(0^\circ)_3$	$(90^\circ)_4$	$(90^\circ)_4$
Case II	1	$(0^\circ)_4$	$(0^\circ)_4$	$(0^\circ)_3$	$(90^\circ)_4$	$(90^\circ)_4$
	2	$(90^\circ)_4$	$(90^\circ)_4$	$(0^\circ)_3$	$(0^\circ)_4$	$(0^\circ)_4$

In order to conveniently describe the delamination between the different layers, the definition of ply number is made by using the model area division of the cross-joint. The layers in UL area, DL area, UR area and DR area are respectively numbered 1 to 4 from the outside to the inside, and the layers in M area number from the left to the right are 1, 2, and 3, respectively. The interface is defined by the layer number and filling area: the layer between the first and second layers in the UL

area is UL1-UL2, and the boundary between fourth layers in UL area and the first layer in M area is defined as UL4-M1-FL.

3.2 The influence of delamination on cross-joint stiffness

The research shows that different lay-ups have obvious effects on the damage and the stiffness of the composite interface. Figure 2 shows the stiffness reduction of interfaces in the scheme 7 of case I, with the increase of load. In the scheme 7 of case I, the interfaces located at the up areas (UL area and UR area) and the boundary of the filling area is more likely to occur delamination damage. As the load increases, the location of deamination damage firstly occurs at DR4-M3-FR, and the bending moment is $396 \text{ N}\cdot\text{mm}$ (0.3 MPa). As the load continues to increase, the stiffness deceleration rate of each interface appears rapidly first and then slowly with continually increasing of the load. When the bending moment increased to $850 \text{ N}\cdot\text{mm}$ (0.6 MPa), the delamination damage began to occur in multiple layers of composites cross-joint, and the stiffness reduction process of each interface was similar to that of DR4-M3-FR.

The relationship between the bending moment and the deformation angle of the bottom wing under the equivalent pressure load is given in Figure 3. Linear relationship between moment and angle at the initial stage of loading ($0\sim 900 \text{ N}\cdot\text{mm}$), indicates the moment angle relation of the connecting structure without delamination damage. With the increase of bending moment, the nonlinear relationship between bending angle and angle is more obvious, and the stiffness of bending moment decreases. Compared with figures 2 and 3, the damage of individual delamination damage has little effect on the bending stiffness of composite cross-joint. When the multiple domination damage are obvious (the stiffness reduction is more than 10%), the bending stiffness of the cross-joint become weakened, and the stiffness of the cross-joint significant decreases with the aggravate increase of the delamination damage.

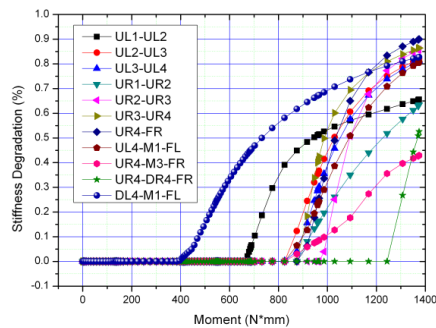


Fig.2. Stiffness reduction between layers in scheme 7 of case I

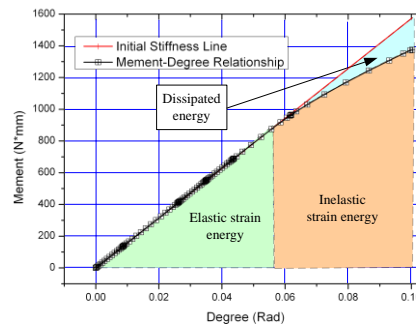


Fig.3. Moment-degree relationship in scheme 7 of case I

4 Analysis of delamination of cross-joint

4.1 Case I: delamination of cross-joint

In the case I, the laminates orientation of UL area, DL area, UR area and DR area (variable area) are the same. The laminates orientation angle increases from 0° to 90° every 15° in the variable area, and laminates orientation is kept 0° in M area (unchanging area). The different ply angle has a significant effect on the delamination damage of the composite cross-joint. It is not difficult to find the damage between different designs of the scheme 1, scheme 4, and scheme 7 (Figure 2, Figure 4, Figure 5). As the laminate orientation angle increases, the initial damage load decreases gradually and the more serious stiffness degradation. When the lay angle is 45 degrees in the various areas, the number of damaged interface of the cross-joint is more than that of 0 degree and 90 degree. Table 5 shows the comparison of damage mechanics property between different situations in design. With the increase of the layer angle, the interfacial dissipated energy and the maximum interface stiffness degradation are grow up gradually, while the initial damage load and displacement decrease gradually. It is indicated that the increase of the layer angle leads to the larger Discontinuities of the interface deformation, and increases the interlaminar stress. The larger interlaminar stress will lead to earlier entry damage stage of the cross-joint. It is not difficult to find the change rule of the parameters from the table. When the laying angle changes from 0 degrees to 45 degrees, the parameters of the interface damage change rapidly. When the laying angle is greater than 45 degrees, with the increase of laying angle, the change of interface damage parameter gradually decreases, and gradually proceeds to that is in scheme of case I.

Table 5. The delamination damage in case I

Scheme	1	2	3	4	5	6	7
laminates orientation	0°	15°	30°	45°	60°	75°	90°
Dissipated energy ($J \cdot 10^{-3}$)	115.47	177.26	237.89	359.65	464.85	485.90	512.53
Initial damage load (<i>MPa</i>)	0.80	0.60	0.53	0.47	0.49	0.48	0.48
Initial damage displacement (<i>mm</i>)	0.37	0.33	0.42	0.44	0.63	0.64	0.64
Max stiffness degradation (%)	59.3	77.2	83.4	86.0	86.2	86.5	87.4

Through comparison and analysis of the damage between seven schemes in case I, it is found that the first delamination damage and the most serious stiffness

degradation occur in the UL area under the 7 schemes in case I . Figure 6 shows the stiffness degradation distribution of the UL1-UL2 fillet region under the seven schemes, and the dotted line shows the boundary of the high damage zone. In scheme 1 and 7, when the laminate orientation is 0 degrees and 90 degrees, the damage zone is distributed evenly along the Y direction. As the laminate orientation approaches to the direction of (1, 1, 0), the stiffness degradation concentration is obvious on the boundary of the cross-joint. The distribution of the stiffness degradation is basically the same as the 1 or 2 directions of the laminate orientation.

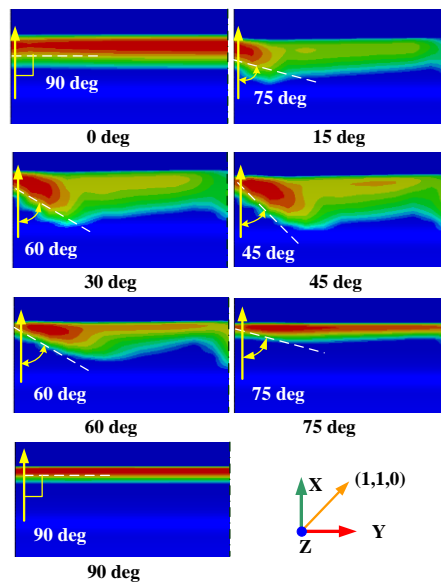


Fig. 6. The distribution of stiffness degradation in the UL1-UL2 fillet region

4.2 Case II : delamination of cross-joint

In case II , the laminates orientation are also kept 0° in M area. The M area is used as middle surface, and the asymmetric lamination orientation design in the two sides of M area. In scheme 1, the fiber direction is 0 degrees in the UL area and DL area, 90 degrees in the UR area and DR area, that is the opposite in the scheme II .Figure 7 shows the stiffness degradation of the cross-joint between the 2 schemes in the case II.

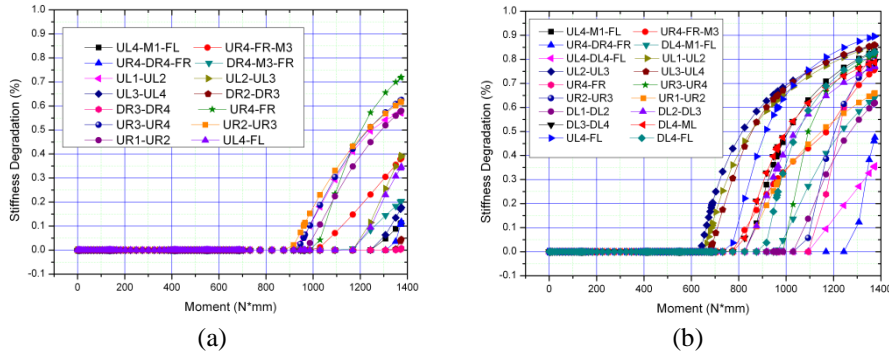


Fig.7. The stiffness degradation of the cross-joint of the 2 schemes in case II.

Table 6. The delamination damage in case II

Scheme	1	2
Dissipated energy (J • 10-3)	503.56	156.13
Initial damage load (MPa)	0.48	0.68
Initial damage displacement (mm)	0.40	0.30
Max stiffness degradation (%)	89.6	72.0

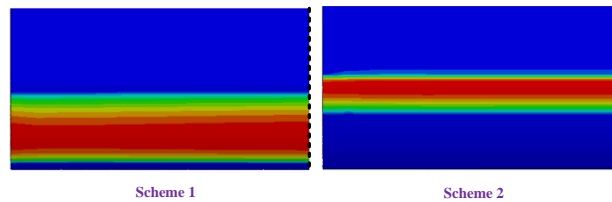


Fig. 7. The distribution of stiffness degradation in the UR1-UR2 fillet region

The reliability of the cross-joint in the scheme 2 is better than in the scheme 1, for the less interface damage, the larger load in the initial damage, and the smaller stiffness reduction. From the location and the extent of the delamination damage of the damage, we can see that the damaged interfaces of UL area and DL area is more than that of UR area and DR area, and the degree of damage is greater in the scheme 1. In contrast to scheme 1, the damage interfaces in the UR area and DR area are more and the degree of damage is greater. By comparing the 2 schemes, the mechanical properties of interlayer damage can be seen (as shown in Table 6). The dissipation energy and the maximum interface stiffness degradation of the cross-joint in scheme 1 are far greater than that in the scheme 2. Figure 7 shows the stiffness degradation distribution cloud chart of UR1-UR2 witch is the large delamination damage. It can be seen that there is no damage concentration in the stiffness degradation distribution along the Y axis of the 2 schemes in case II, and

the position of the high damage area in the 2 schemes is different because of the different layer design.

5 Conclusions

In this paper, an aero-engine composite joint structure is studied and a cross-joint structure is proposed. The effect of layer angle and layer form on delamination damage of the composite cross-joint under the action of equivalent aerodynamic bending are analyzed by finite element method. The following conclusions are obtained:

The laminates orientation has an obvious influence on the degree of delamination damage and the damage distribution of the composite cross-joint, and the delamination damage of the composite structure is mainly in the filleting area between the filling resin area and the laminate area. At the same time, the delamination damage can lead to the bending stiffness reduction of the composite cross-joint, while the damage to the individual interface has little effect on the bending stiffness of the cross-joint structure. When the multiple interfaces are obviously damaged (the stiffness reduction is greater than 10%), the bending stiffness of the cross-joint is weakened and the cross-joint bending stiffness is obviously weakened with the aggravated damage of the interface.

The reliability of composite cross-joint structure which is symmetrical design (case II) decreases with the increase of the laying angle of the variable layer. When the variable area is laid not 0 degrees and 90 degrees, the damage distribution of the connecting structure appears to be concentrated in the boundary. For asymmetrical design (case I) composite cross-joint structure, increasing the stiffness of the pressure side laminates is helpful to alleviate the damage in the interface, and can improve the bending stiffness of the composite cross-joint structure.

The damage distribution of the composite cross-joint structure is basically the same as that of the stress distribution, and the delamination damage is higher in the high stress area. Therefore, by changing the lay angle design and controlling the stress of the cross-joint structure will help to alleviate the damage in interface. According to the above analysis, in practical engineering, the stiffness of the pressure side can be increased by using the asymmetric (case I) ply method according to the load of cross-joint.

References

1. N.B. Yang, Y.N Zhang, *Design of aircraft composite structure*, Aviation Industry Press, Beijing, 2002.
2. H.J. Phillips, R.A. Sheno, Damage tolerance of laminated tee joints in FRP structure, *Composites Part A: Applied Science and Manufacturing*, 29(1998) 465-478.
3. L. Burns, A.P. Mouritz, D. Pook, S. Feih, Strength improvement to composite T-joints under bending through bio-inspired design, *Composites part A*, 43(2012) 1971-1980.

4. M.L. Benzeggagh, M. Kenane, Measurement of Mixed-Mode Delamination Fracture Toughness of Unidirectional Glass/Epoxy Composites with Mixed-Mode Bending Apparatus, *Composites Science and Technology*, 56(1996)439-449.
5. Y.H. Yang, Z.G. Zhou, Y. Gou, Effect of defects on mechanical properties of single joint adhesive joint, *Journal of composite materials*, 29(2012) 157-163.
6. L. Tong, G.P. Stevens, Analysis and design of structural bonded joints, *MA: Kluwer Academic Publishers*, Hingham, 1999.
7. S. Kumari, P. Sinha, Finite element analysis of composite wing T-joints, *Journal of Reinforced Plastics & Composites*, 21(2002) 1561-1585.
8. H. Li, F. Dharamawan, I. Herszberg, S. John, Fracture behavior of composite maritime T-joints, *Composite Structures*, 75(2006)339-350.
9. E. Greenhalgh, A. Lewis, R. Bowen, M. Grassi, Evaluation of toughening concepts at structural features in CFRP—Part I: Stiffener pull-off, *Composites Part A Applied Science & Manufacturing*, 37(2006)1521-1535.
10. A. Orifici, S.A. Shah, I. Herszberg, A. Kotler, T. Weller, Failure analysis in postbuckled composite T-sections, *Composite Structures*, 86(2008) 146-153.
11. A. Dodkins, R. Sheno, G. Hawkins, Design of joints and attachments in FRP ships' structures, *Marine Structures*, 7(1994)365-398.
12. J. Dulieu-Barton, J. Earl, R. Sheno, Determination of the stress distribution in foam-cored sandwich construction composite tee joints, *Journal of Strain Analysis for Engineering Design*, 36(2001,) 545-560.
13. R. Sheno, P. Read, G. Hawkins, Fatigue failure mechanisms in fibre-reinforced plastic laminated tee joints, *International Journal of Fatigue*, 17(1995) 415-426.
14. J.M. Dulieu-Smith, S. Quinn, R.A. Sheno, Thermoelastic stress analysis of a GRP tee joint, *Applied Composite Materials*, 4(1997)283-303.
15. Sheno R, Hawkins G. Influence of material and geometry variations on the behaviour of bonded tee connections in FRP ships, *Composites A*, 23(1992)335-345.
16. E.G. Koricho, G. Belingardi, An experimental and finite element study of the transverse bending behaviour of CFRP composite T-joints in vehicle structures, *Composites Part B*, 79(2015)430-443.
17. S. Akpınar, M.D. Aydın, T. Şemsettin, 3-D non-linear stress analysis on the adhesively bonded T-joints with embedded supports, *Composites Part B Engineering*, 53(2013) 314-323.
18. D.W Zhou, L.A. Louca, M.Saunders, Numerical simulation of sandwich T-joints under dynamic loading, *Composites Part B Engineering*, 39(2008)973-985..
19. H. Wu, J. Xiao, S. Xing, S. Wen, F. Yang, J. Yang, Numerical and experimental investigation into failure of T700/bismaleimide composite T-joints under tensile loading, *Composite Structures*, 130(2015)63-74.
20. S.C. Avalon, S.L. Donaldson, Strength of composite angle brackets with multiple geometries and nanofiber-enhanced resins, *Journal of Composite Materials*, 45(2010), 1017-1030.